

# Using eddy covariance observations to determine the carbon sequestration characteristics of subalpine forests in the Qinghai-Tibet Plateau

Niu Zhu<sup>1,2,4</sup>, Jinniu Wang<sup>1,2</sup>, Dongliang Luo<sup>3</sup>, Xufeng Wang<sup>3</sup>, Cheng Shen<sup>1,2</sup>, Ning Wu<sup>1</sup>

<sup>1</sup>Chengdu Institute of Biology, Chinese Academy of Sciences, Chengdu 610041, China

<sup>2</sup>Mangkang Ecological Monitoring Station, Tibet Ecological Security Barrier Ecological Monitoring Network, Qamdo 854500, China

<sup>3</sup>Northwest Institute of Eco-environmental Resources, Chinese Academy of Sciences, Lanzhou 730000, China

<sup>4</sup>College of Resources and Environmental Sciences, Gansu Agricultural University, Lanzhou 730070, China

*Correspondence:* Jinniu Wang (wangjn@cib.ac.cn)

**Abstract:** The subalpine forests are a crucial component of the carbon cycling system in the Qinghai-Tibet Plateau (QTP). However, there are significant data gaps in the QTP currently, it also essential to enhance continuous monitoring of forest carbon absorption processes in the future. This study investigates two years' carbon exchange dynamics of a subalpine forest on the QTP using the eddy covariance method. We first characterized its seasonal carbon dynamics of the subalpine forest, revealing the higher carbon dioxide exchange rates in summer and autumn and lower rates in winter and spring, and found that autumn is the peak period for carbon sequestration in the subalpine forest, with the maximum measured value of CO<sub>2</sub> absorption reaching 10.70  $\mu\text{mol m}^{-2} \text{s}^{-1}$ . Subsequently, we examined the environmental factors influencing carbon sequestration function. The PCA analysis show that photosynthetically active radiation (PAR) was major environmental factor driving the net ecosystem CO<sub>2</sub> exchange (NEE), significantly influencing forest and carbon absorption, and the increase of relative humidity decreases the rate of carbon fixation. In addition, we explored NEE and its influencing factors at the regional scale, found that air temperature promotes carbon dioxide absorption (negative NEE values), while the average annual precipitation shows a minor effect on NEE. At the annual scale, the subalpine forest functions as a strong carbon sink, with an average NEE of  $-332\sim-351 \text{ g C m}^{-2}$  (from November 2020 to October 2022). Despite facing the challenges of climate change, forests remain robust carbon sinks with the highest carbon sequestration capacity in the QTP, with an average annual CO<sub>2</sub> absorption rate of 368  $\text{g C m}^{-2}$ . This study provides valuable insights into the carbon cycling mechanism

31 in subalpine ecosystems and the global carbon balance.

32 **Keywords:** Subalpine forest; Qinghai-Tibet Plateau; The eddy covariance method; Three Parallel Rivers  
33 Region; Carbon sinks

## 34 **1 Introduction**

35 Carbon dioxide (CO<sub>2</sub>) is a prominent greenhouse gas, and its atmospheric concentration has reached an  
36 unprecedented high level in recent years, in May 2021, a recorded peak of 419 parts per million (ppm)  
37 was observed at the Mauna Loa Observatory in Hawaii (Stein, 2021). The global atmospheric CO<sub>2</sub>  
38 concentration is rapidly increasing at a rate of 2 to 3 ppm per year, compared to pre-industrial levels, the  
39 average global temperature has already risen by 1.1 °C by 2019 (World Meteorological Organization,  
40 2019). Human activities have been the primary catalyst behind the significant surge in atmospheric CO<sub>2</sub>  
41 concentrations (Schweizer et al., 2020). CO<sub>2</sub> and CH<sub>4</sub> collectively contribute approximately 70% to the  
42 global warming potential among the six greenhouse gases specified in the Kyoto Protocol (Zhang et al.,  
43 2022). As atmospheric CO<sub>2</sub> concentrations continue to rise, global climate warming is gradually  
44 intensifying. Therefore, The Paris Agreement urges national governments to restrict the increase in  
45 global average temperature to well below 2.0 °C above pre-industrial levels and to strive to limit it to  
46 1.5 °C. The increasing atmospheric CO<sub>2</sub> levels will lead to irreversible ecological disasters. For instance,  
47 the concentration of CO<sub>2</sub> in the atmosphere is projected to double within approximately 50 years if global  
48 consumption of fossil fuels continues to rise at the current rate. Addressing the greenhouse effect caused  
49 by carbon dioxide and reducing its impact is a crucial challenge facing human society today. Reducing  
50 regional carbon emissions or per capita carbon emissions is widely regarded as an effective approach to  
51 carbon reduction (Wang et al., 2023a). Nevertheless, countries around the world have already begun to  
52 commit to carbon reduction and carbon neutrality efforts. On September 22, 2020, during the 75th session  
53 of the United Nations General Assembly, the Chinese government announced "double carbon" goals,  
54 which aim to achieve carbon emission peaking by 2030 and carbon neutrality by 2060, in alignment with  
55 ecological conservation and sustainable development objectives (Yu, 2022). It is predicted that China's  
56 average forest carbon sequestration rate will reach 0.358 Pg C year<sup>-1</sup> by 2060 (Cai et al., 2022). This  
57 significant rate of carbon sequestration is expected to have a substantial impact on the environment and  
58 economy, providing negative feedback to global warming (Pan et al., 2011).

59 Currently, there are various methods available to accurately quantify the carbon sequestration potential  
60 of forests. Quantitative estimation of carbon sequestration potential still requires scientists to establish  
61 more *in-situ* sites and generate comprehensive datasets to assess a wide range of areas. Initially,  
62 individuals' biomass measurements were used to estimate forest carbon sequestration capacity  
63 (Ebermayer, 1876). However, this method was time-consuming, labor-intensive, and prone to  
64 inaccuracies due to the omission of various variables during the calculation process. The development  
65 of modeling techniques allowed for the use of simulation methods-forest management models and land  
66 ecosystem-climate interaction models, such as the Ecological Assimilation of Land and Climate  
67 Observation (EALCO), have been widely applied in this regard (Landsberg and Waring, 1997; Wang et  
68 al., 2001). Currently, remote sensing monitoring and the eddy covariance (EC) method are quite popular.  
69 Remote sensing techniques can be used to extract vegetation parameters (e.g., normalized difference  
70 vegetation index (NDVI)) from multispectral bands and estimate the carbon sequestration of entire  
71 forests through regression analysis (Laurin et al., 2014). The eddy covariance method, allowing  
72 continuous, long-term carbon flux calculation, provides fundamental data for model establishment and  
73 calibration. It has been widely applied across ecosystems, including urban areas, farmlands, grasslands,  
74 forests, and water bodies (Konopka et al., 2021; Vote et al., 2015; Du et al., 2022a; Kondo et al., 2017;  
75 Li et al., 2022).

76 The forest ecosystem's Net ecosystem exchange (NEE) of carbon dioxide is influenced by multiple  
77 environmental factors. Previous studies have shown that NEE is significantly influenced by air  
78 temperature (AT), photosynthetically active radiation (PAR), vapor pressure deficit (VPD), relative  
79 humidity (RH), and soil temperature (ST) (Liu et al., 2022). For instance, temperature variables,  
80 especially annual or seasonal average temperature variations, serve as the optimal single predictor for  
81 carbon flux, explaining variations in carbon flux between 19% and 71% (Banbury Morgan et al., 2021).  
82 PAR not only influences the absorption of carbon dioxide by the forest canopy but also affects the  
83 utilization of carbohydrates by roots due to its association with canopy processes and soil respiration  
84 (Baumgartner et al., 2020). Furthermore, research suggests that NEE is influenced by biotic factors such  
85 as NDVI and leaf area index (LAI) (Tang et al., 2022). Given the projected future global warming trends,  
86 forests play a highly significant vast carbon reservoir for their becoming worthy of attention. The  
87 Qinghai-Tibet Plateau (QTP) is the highest and largest plateau in the world, with an extensive area of

88 alpine forests covering approximately  $2.3 \times 10^5 \text{ km}^2$ , holding tremendous economic and ecological  
89 benefits. The southeastern region of the QTP boasts one of the world's highest-altitude subalpine forest  
90 ecosystems. Research indicates that the subalpine forest ecosystem in this area has a remarkable capacity  
91 to consume methane, reaching up to  $5.06 \text{ kg ha}^{-1} \text{ yr}^{-1}$ , and playing a significant role in mitigating the  
92 impact of greenhouse gases (Qu et al., 2023). Since the 1960s, the QTP has experienced a faster warming  
93 rate than lowland areas, a phenomenon projected to intensify by the end of the 21st century (Li et al.,  
94 2019). Currently, the QTP is considered a weak carbon sink at the overall level, but the carbon source-  
95 sink dynamics vary among different ecosystems (Chen et al., 2022). For instance, most lakes in the QTP  
96 are currently characterized by supersaturated  $\text{CO}_2$  levels (Cole et al., 1994). Mu et al. (2023) found that  
97 the thermokarst lakes serve as significant carbon sources through carbon flux measurements in 163  
98 thermokarst lakes during the summer and autumn seasons. Wang et al. (2021) discovered that by  
99 comparing carbon fluxes in ten high-mountain ecosystems with different grassland types, these  
100 ecosystems act as sinks for carbon dioxide. The alpine meadows in the eastern QTP were identified as  
101 strong carbon sinks, with the highest annual average NEE recorded at  $-284 \text{ g C m}^{-2}$ . Forest ecosystems  
102 play a crucial role in the southeastern edge of the QTP, providing important support for climate regulation  
103 and forestry-based economic activities. Moreover, recent predictive studies suggest that under both  
104 current and future climate scenarios, the forested area in this region is expected to expand further, with  
105 coniferous forests continuing to grow into higher altitudes (Liu et al., 2021). Due to the extensive  
106 presence of permafrost in the QTP, forest net primary productivity exhibits a most pronounced response  
107 to surface temperatures in the continuous permafrost zone over multiple years. Therefore, the changes in  
108 permafrost in the QTP should not be overlooked, as they also have a significant impact on carbon  
109 absorption by forests (Mao et al., 2015). However, the QTP is a vast region with a widespread distribution  
110 of high-altitude and subalpine forests. Long-term monitoring is necessary to understand how these forests  
111 will respond to climate change. Furthermore, there is a significant data gap concerning the monitoring of  
112 carbon exchange capacity in the forests of the QTP, indicating the need for further data collection efforts.  
113 Based on this, we established a carbon flux monitoring site in the subalpine ecosystem of the Three  
114 Parallel Rivers Region, which is located on the southeastern edge of the QTP and is renowned as a global  
115 hotspot for biodiversity (Wang et al., 2022a). Our research objectives are to:

- 116 1) Determine whether the subalpine forests in the Three Parallel Rivers Region act as a carbon sink or  
117 source, and quantify the annual uptake or release of carbon dioxide;
- 118 2) Investigate the influences of main environmental factors on the carbon exchange process in the  
119 subalpine forests and identify the factors with the greatest impact, and;
- 120 3) Evaluate the carbon exchange capacity of subalpine forests in the QTP by comparing existing data  
121 with other ecosystems in the region.

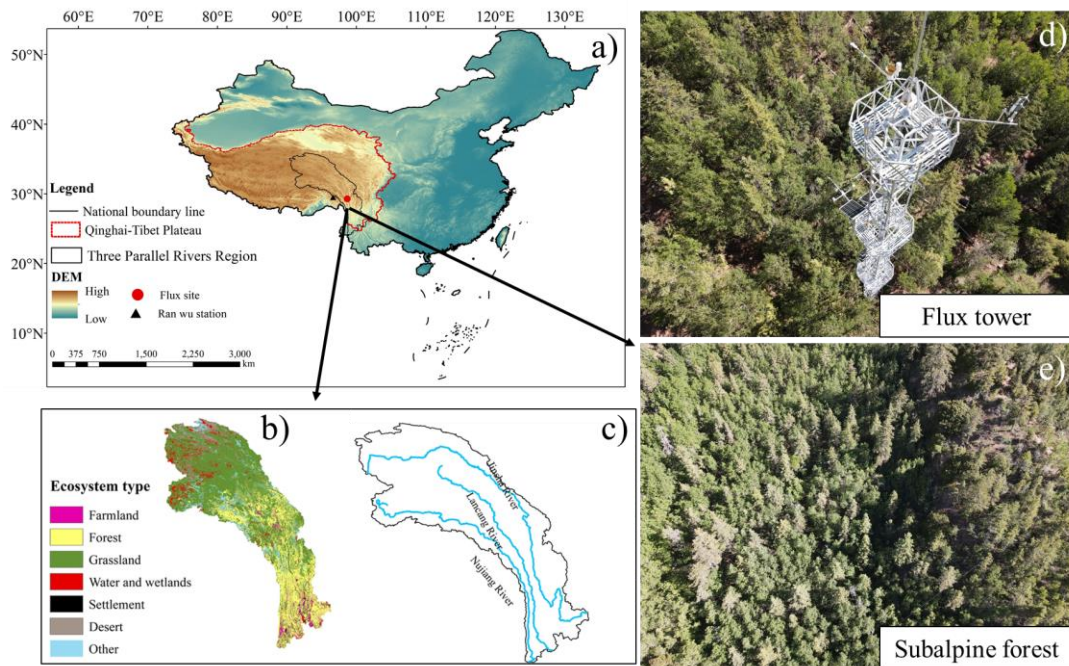
122 This study will provide a data foundation and background support for accurately estimating the carbon  
123 balance of forests in high-altitude areas and for model simulations in the future.

## 124 **2 Materials and Methods**

### 125 **2.1 Overview of the study site**

126 The study site is located in the Hongla Mountain Yunnan Snub-nosed Monkey National Nature Reserve  
127 in Mangkang County, Tibet, China (29°17'10.78"N, 98°41'27.45"E), the core area of the watershed of  
128 the Three Parallel Rivers (Nujiang River, Lancang River, and Jinsha River). The elevation of the study  
129 site is 3755 m. The observation period was from November 2020 to October 2022. The study area  
130 experiences large diurnal temperature variations and dry conditions in winter, while the summers are  
131 warm and humid. The average daily sunshine duration exceeds 10 h, with an annual average temperature  
132 of 5 °C and an average annual precipitation of around 600 mm within a year (Niu et al., 2023). The main  
133 tree species in the area include *Picea likiangensis* var. *rubescens*, *Abies squamata*, *Sabina tibetica* Kom,  
134 and *Abies ernestii*. They are accompanied by the growth of some *Quercus aquifolioides*, *Rhododendron*  
135 *lapponicum*, and *Potentilla fruticosa* shrubs. The average height of the trees is around 30 m, and the  
136 forest is in a relatively active growth phase, reaching the state of a mature forest. The vegetation coverage  
137 ranges from 70% to 80%. The dominant soil type is yellow-brown soil. The mountainous terrain  
138 contributes to distinct vertical climate characteristics and significant variations in water and heat  
139 conditions, with numerous dry and hot river valleys, widespread canyons, and a clear impact from the  
140 southwest and southeast monsoons. The varying elevations give rise to diverse ecosystems, transitioning  
141 from alpine forests to mountain shrubs. Above 4000 m asl, high alpine grasslands and meadows form a  
142 noticeable vegetation transition zone. The mountainous topography results in distinct vertical climate

143 features and significant fluctuations in water and heat conditions, with precipitation showing a markedly  
144 uneven distribution throughout the study region (Zemin et al., 2023).



145  
146 **Figure 1: Location of the flux site (a). Ecosystem types (b) and main rivers (c) in the Three Parallel Rivers**  
147 **Region. Flux tower (d) and forest top view (e).** (The national boundary range in the figure was retrieved from  
148 <http://bzdt.ch.mnr.gov.cn>, and elevation data and ecosystem type are from [www.gscloud.cn](http://www.gscloud.cn)).

149

## 150 2.2 Eddy covariance system

151 The EC system is deployed at a 35 m-high tower located at the study site. At the top of the tower, a 3-D  
152 wind velocity (Wind Master, Gill, UK) and an open-path infrared CO<sub>2</sub>/H<sub>2</sub>O analyzer (LI-7500DS, Li-  
153 Cor, USA) were installed to measure CO<sub>2</sub> flux. The instruments had a measurement frequency of 10 Hz.  
154 Additionally, micro-meteorological sensors were placed at different heights on the tower, including  
155 sensors at 35 m for observing air temperature and humidity (HMP155A, Vaisala, Finland), sensors at -5  
156 cm for soil temperature (TEROS11, LI-Cor, USA), and sensors at 35 m for photosynthetically active  
157 radiation (LI-190R, LI-Cor, USA). All data was stored for 30-minute in a SmartFlux 3 data logger (Li-  
158 Cor, USA) for future download.

## 159 2.3 Data processing and quality control

160 When considering only the turbulent transport of matter and energy in the vertical direction, the carbon  
161 dioxide flux ( $F_c$ ) can be represented by the following equation (Yu and Sun, 2006; Monteith et al., 1994):

162  $F_c = \overline{W'CO_2'}$  (1)

163 Where  $W'$  is the vertical component of 3-D wind speed fluctuations ( $m\ s^{-1}$ ), and  $CO_2'$  represents the  
164 fluctuations in measured  $CO_2$  mole concentration. A positive  $F_c$  indicates carbon emissions, while a  
165 negative value represents carbon uptake.

166 The acquired 10 Hz raw data was processed and corrected using the EddyPro software (EddyPro 7.06,  
167 Li-Cor, USA). The calibration process involved outlier detection for flux data, lag elimination, coordinate  
168 rotation (Jia et al., 2020), ultrasonic temperature correction (Schotanus et al., 1983), frequency correction  
169 (Moncrieff et al., 1997), and Webb-Pearman-Leuning (WPL) correction (Leuning and King, 1992). After  
170 these controls, the integrity of the effective FC raw data we obtained reached 92.95 %. We removed  
171 outliers caused by environmental disturbances such as power outages, rain, snow, and dust particles that  
172 interfered with the instrument. Due to the slope of the underlying surface being around 5 degrees, we  
173 also corrected from non-uniform and non-flat surfaces using EddyPro for double-coordinate rotation  
174 (Cao et al., 2019). As a result, we obtained half-hourly flux data with associated data quality indicators.  
175 To evaluate the turbulence steadiness, we employed the "0-1-2" quality assessment method, which  
176 classified flux results into three quality levels: 0 for excellent data quality, 1 for moderate data quality,  
177 and 2 for low data quality (Mauder and Foken, 2011; Foken et al., 2005). We removed data points labeled  
178 with a quality level of "2". We further eliminated flux data with negative values during nighttime since  
179 plants do not perform photosynthesis at night. Additionally, we conducted spectral analysis to identify  
180 and remove data points with values significantly deviating from normal. Finally, friction velocities ( $u^*$ )  
181 for each of the two years were determined separately using the method of moving point, and deleted data  
182 recorded during nighttime when  $u^*$  was less than 0.28 and 0.39  $m\ s^{-1}$  (Reichstein et al., 2005). After  
183 excluding outliers from the data, the data integrity is 72.67%. Tovi software (Tovi, Li-Cor, USA) was  
184 used in the process.

185 When turbulence is weak, a portion of  $CO_2$  is stored in the vegetation canopy and the atmosphere below  
186 the measurement height. At this time, the NEE is calculated as (Zhang et al., 2018):

187  $NEE = F_c + F_s$  (2)

188 Where NEE represents the net ecosystem exchange of  $CO_2$ ,  $F_c$  stands for the observed flux during a  
189 specific period,  $F_s$  represents the  $CO_2$  storage in the forest canopy,  $F_s$  is calculated as  $(\Delta c/\Delta t) \cdot h$ , where

190  $\Delta c$  is the difference in CO<sub>2</sub> concentration between two consecutive measurements,  $\Delta t$  is the time interval  
191 between two consecutive measurements, and  $h$  is 35 m.

192 We adopted the following formula as a gap-filling strategy for daytime NEE ( $NEE_{\text{day}}$ ) concerning PAR,  
193 aiming to address missing values during the daytime (Falge et al., 2001):

$$194 \quad NEE_{\text{day}} = \frac{\alpha \times \text{PAR} \times P_{\text{max}}}{\alpha \times \text{PAR} + P_{\text{max}}} - R_{\text{day}} \quad (3)$$

195 where  $\alpha$  ( $\mu\text{mol CO}_2/\mu\text{mol PAR}$ ) represents the apparent photosynthetic quantum efficiency, which  
196 characterizes the maximum efficiency of converting light energy during photosynthesis; PAR ( $\mu\text{mol m}^{-2}$   
197  $\text{s}^{-1}$ ) is the photosynthetically active radiation, a measure of the amount of light energy available for  
198 photosynthesis;  $P_{\text{max}}$  ( $\mu\text{mol CO}_2 \text{ m}^{-2} \text{ s}^{-1}$ ) is the apparent maximum photosynthetic rate, representing the  
199 maximum CO<sub>2</sub> uptake rate under optimal conditions, and;  $R_{\text{day}}$  ( $\mu\text{mol CO}_2 \text{ m}^{-2} \text{ s}^{-1}$ ) is the daytime dark  
200 respiration rate, which denotes the rate of CO<sub>2</sub> release during daylight hours.  $\alpha$ ,  $P_{\text{max}}$ , and  $R_{\text{day}}$  are obtained  
201 through the non-linear fitting of the Michaelis-Menten model to the observed data.

202 During the nighttime, the NEE is modeled using an exponential function of ecosystem respiration and  
203 soil temperature to fill in the missing values of NEE during the night ( $NEE_{\text{night}}$ ) (Lloyd and Taylor, 1994;  
204 Kato et al., 2006):

$$205 \quad NEE_{\text{night}} = a \times \exp(bt) \quad (4)$$

206 Where  $a$  and  $b$  are estimated values for the exponential function used in modeling  $NEE_{\text{night}}$ , and;  $t$   
207 represents the soil temperature measured at the depth of 5 cm. Origin 2023 (Originlab Corporation, USA)  
208 is the data processing software used for this analysis. For the missing data, interpolation was performed  
209 using Tovi software allows for data interpolation to fill in the gaps and ensure a continuous dataset for  
210 further analysis (Reichstein et al., 2005). 27.33% of missing data were interpolated using Tovi after  
211 filtering, resulting in a flux data set with complete data integrity.

212 In flux analysis, the significance of source area contributions cannot be overlooked. In this study, the  
213 peak distances of the 90% flux contribution areas averaged over two years are 364.2 and 357.1m,  
214 respectively. In terms of seasons, the average peak distances of the 90% flux contribution areas for winter,  
215 spring, summer, and autumn over the two years are as follows: 353.9, 358.2, 350.05, and 344.34m,  
216 respectively.

## 217 **2.4 Flux partitioning**



218 Ecosystem respiration (RE) is the sum of plant and heterotrophic respiration in an ecosystem and is  
219 obtained by adding the measured nighttime data to the extrapolated daytime data. Gross primary  
220 productivity (GPP) is the total amount of organic carbon fixed by green plants through photosynthesis  
221 per unit of time and per unit of area:

$$222 \quad RE = R_{\text{day}} + R_{\text{night}} \quad (5)$$

$$223 \quad GPP = -NEE + RE \quad (6)$$

224 Carbon use efficiency (CUE) is a crucial parameter that reflects the ability of an ecosystem to sequester  
225 carbon. It is defined as the ratio of net ecosystem productivity (NEP) to gross primary productivity. CUE  
226 can be expressed using the following equation:

$$227 \quad CUE = \frac{NEP}{GPP} = \frac{-NEE}{GPP} \quad (7)$$

228 To study the variation of ecosystem respiration rates with environmental factors, we considered the  
229 dependence of nocturnal ecosystem respiration on soil temperature (Pavelka et al., 2007; Mamkin et al.,  
230 2023):

$$231 \quad Q_{10} = \exp(10 \times \alpha) \quad (8)$$

$$232 \quad \ln(NEE_{\text{night}}) = \alpha \times T \times \gamma \quad (9)$$

233 Where T is the soil temperature (°C) and  $\gamma$  is an empirical parameter of the equation.

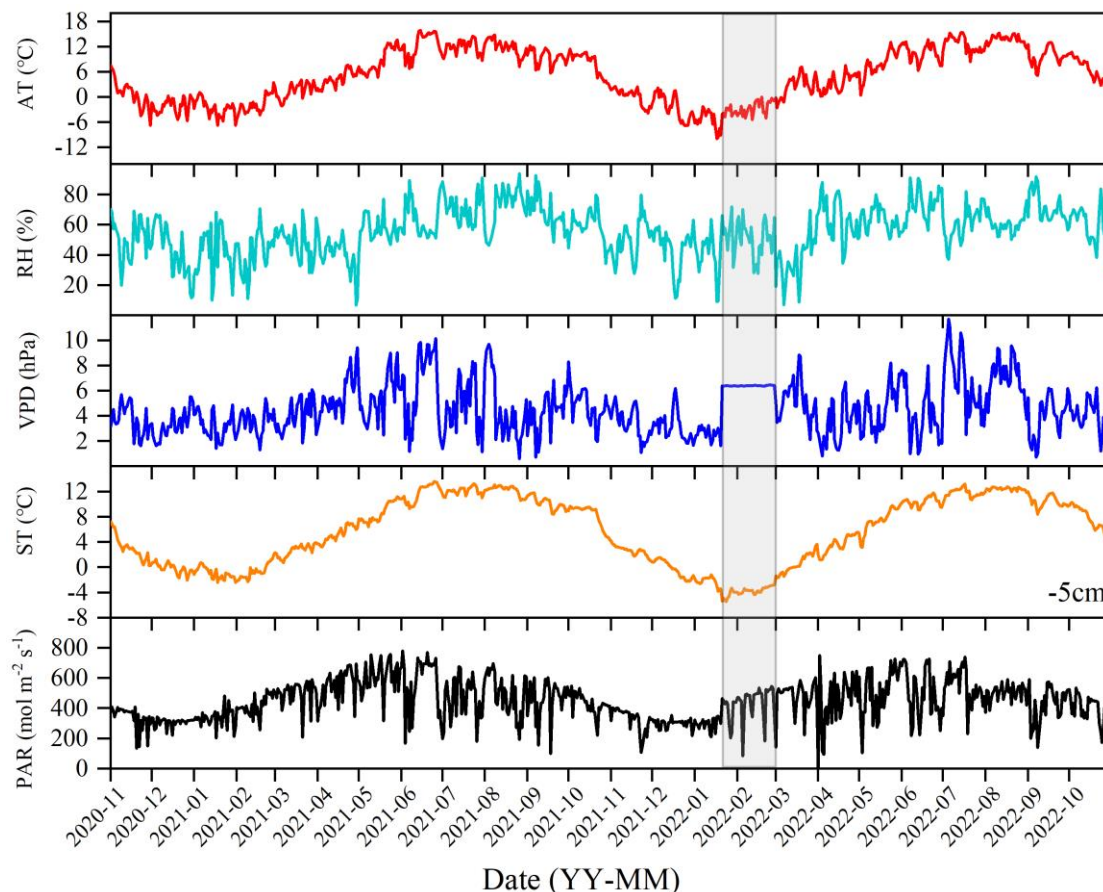
234 To clarify the carbon sink potential of forests in the QTP and to compare it with other ecosystems, a  
235 search was conducted in two authoritative databases, Web of Science and China National Knowledge  
236 Internet, for research articles on the current utilization of EC systems in the QTP. A total of 82 research  
237 results were collected from 48 studies, and their annual average environmental factors, such as air  
238 temperature, precipitation, and altitude, were obtained.

## 239 **3 Results**

### 240 **3.1 Daily changes in main environmental factors**

241 During the observational period, the environmental conditions exhibited significant fluctuations. The  
242 winter and spring seasons were characterized by cold and dry conditions, while the summer and autumn  
243 seasons were warm and humid. The daily maximum AT recorded was 15.87 °C (on June 15, 2021), and  
244 the minimum temperature was -9.88 °C (on January 17, 2022), with a mean annual average of 5.5 °C  
245 over the two years. RH is averaged at 55.89%, and VPD is averaged at 4.46 hPa. ST exhibited a similar

246 trend to air temperature. The highest observed soil temperature was 13.53 °C (on June 27, 2021), while  
 247 the minimum was -3.78 °C (on January 18, 2022), with an annual average of 6.11 °C. PAR is averaged  
 248 at 447.24 mol m<sup>-2</sup> s<sup>-1</sup>.



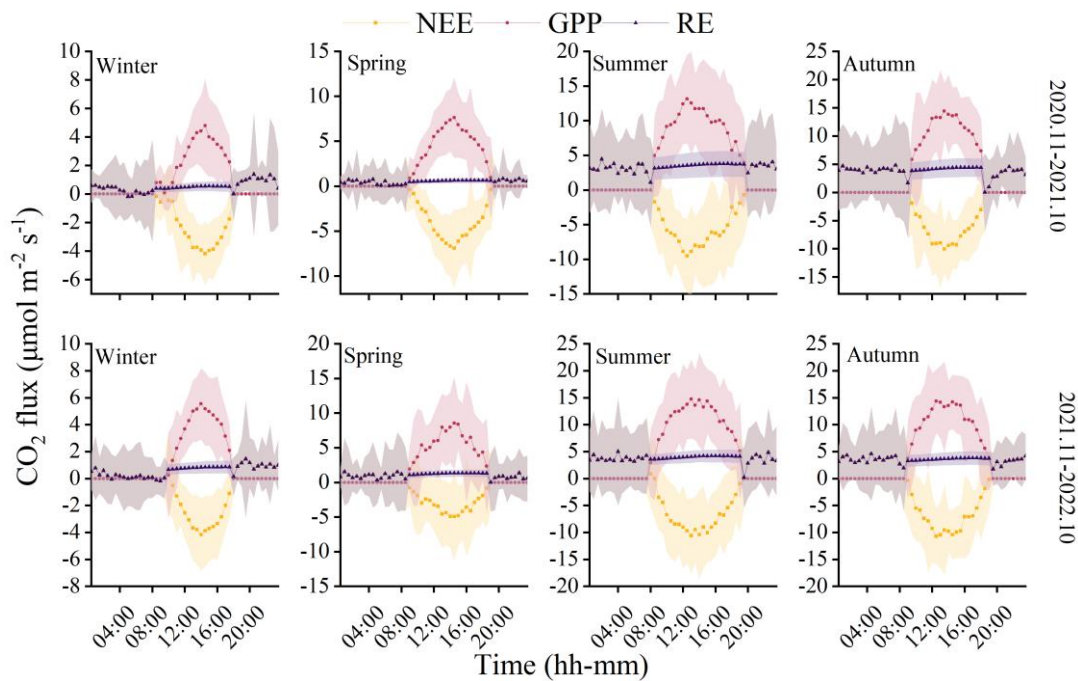
249  
 250 **Figure 2: Daily values of main environmental factors, air temperature (AT), relative humidity (RH), vapor**  
 251 **pressure deficit (VPD), soil temperature (ST), and photosynthetically active radiation (PAR).** (The data of the  
 252 **shadow part in the figure comes from the Ranwu forest site (Figure 1). Since there was no interpolated data**  
 253 **source for VPD, the annual average was used instead.).**

254

### 255 3.2 Seasonal dynamics of NEE, RE, and GPP

256 The observations from the forest ecosystem indicate distinct diurnal and seasonal variations in NEE and  
 257 GPP (Figure 3). The NEE and GPP exhibit a pronounced U-shaped curve, with significant seasonal  
 258 differences. The summer and autumn are characterized by peak carbon uptake, with the maximum NEE  
 259 reaching. During the nighttime, the ecosystem generally releases carbon, while during favorable daytime  
 260 meteorological conditions, it demonstrates a carbon uptake capacity. The peak carbon absorption of the  
 261 forest ecosystem occurs from 12:00 to 15:00 (Beijing time, UTC+8:00). The daily carbon sequestration

262 in summer and autumn is 1.5-3 hrs longer than in winter. The timing of maximum carbon sequestration  
 263 capacity changes with each season. In winter, the transition from nighttime carbon release to daytime  
 264 carbon uptake occurs around 08:30, which is approximately 1 hour later than in summer. GPP  
 265 characterizes the forest's carbon sequestration capacity, and since photosynthesis does not occur at night,  
 266 GPP is zero during nighttime. The maximum daily total productivity is recorded at  $14.76 \pm 7.34 \mu\text{mol}$   
 267  $\text{CO}_2 \text{ m}^{-2} \text{ s}^{-1}$  during the summer of the second year, with a standard deviation indicating greater variability  
 268 in GPP and NEE during the summer and autumn compared to the winter and spring. Although diurnal  
 269 variations in RE are relatively small, there are significant seasonal differences. During the night, when  
 270 only respiration occurs, RE equals NEE. However, as photosynthesis becomes active during the day, RE  
 271 gradually increases and stabilizes. The respiratory rate of the coniferous forest is highest in autumn, being  
 272 eight times greater than in winter.



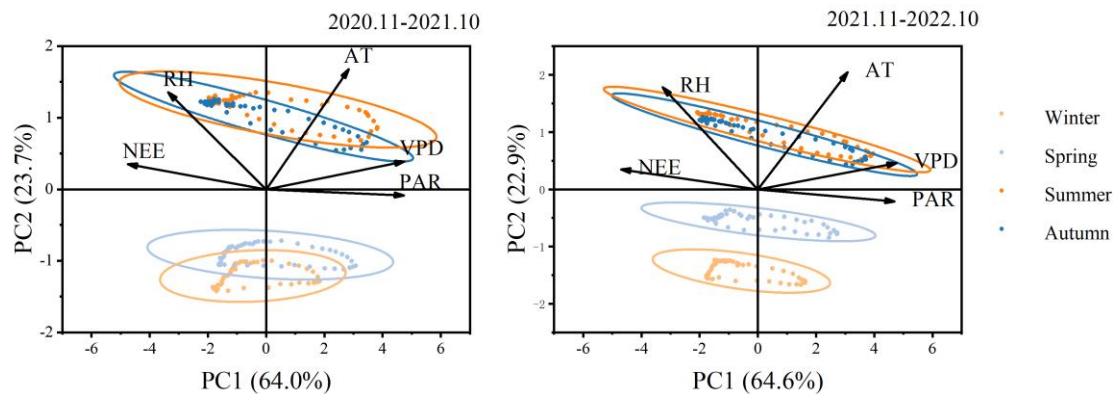
273  
 274 **Figure 3: Monthly mean values of CO<sub>2</sub> fluxes.**

275

### 276 3.3 Relationship between NEE and main environmental factors

277 The PCA analysis of NEE and environmental factors (Figure 4) indicates that the explanations for the  
 278 first principal component (PC1) and the second principal component (PC2) are essentially the same  
 279 between the two years. The total contributions of PC1 and PC2 are 87.7% and 87.5%, respectively, with  
 280 PC1 accounting for 64.0% and 64.6% individually. The angle between photosynthetically active

281 radiation (PAR) and PC1 is minimal, suggesting a strong correlation between PAR and PC1. Additionally,  
 282 PAR and VPD contribute the most to PC1, while AT and RH contribute the most to PC2. The analysis  
 283 results reveal a significant positive correlation between NEE and RH, while a significant negative  
 284 correlation is observed with AT, VPD, and PAR. Increased RH is detrimental to forest carbon dioxide  
 285 absorption. Excessively high relative humidity causes plant leaf stomata to close, reducing the amount  
 286 of carbon dioxide available to the plant. This, in turn, leads to a decrease in the efficiency of carbon  
 287 fixation through photosynthesis. Among these environmental factors, PAR plays a dominant role.  
 288 Furthermore, the figure illustrates the relationships between environmental factors, showing a positive  
 289 correlation between RH and TA, and a negative correlation with VPD and APR. The indicators exhibit  
 290 some seasonality, with notable differences between the winter-spring and summer-autumn seasons,  
 291 indicating limited similarity between seasons.

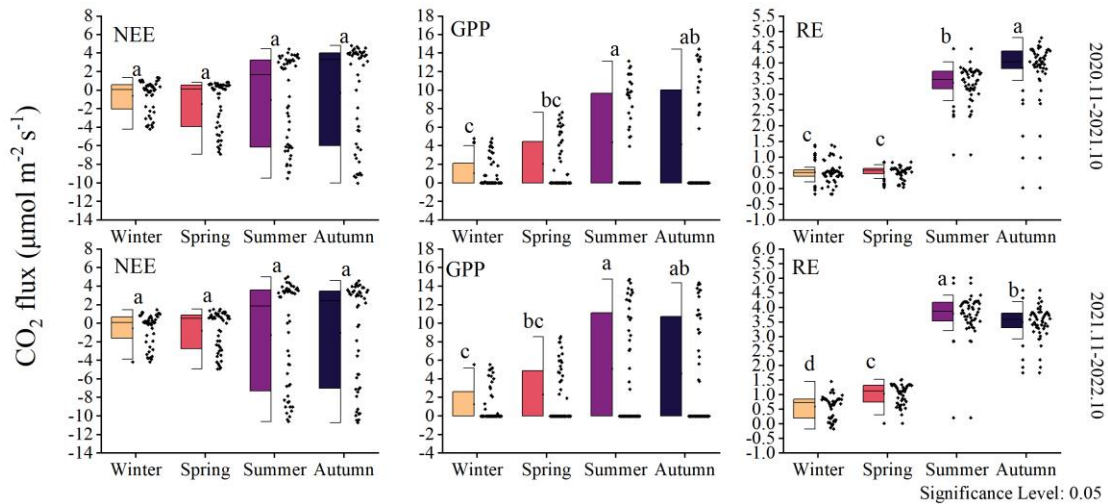


292  
 293 **Figure 4: Principal component analysis of environmental factors and NEE.**

294

### 295 3.4 Seasonal variation of NEE, GPP, and RE

296 The NEE did not show significant inter-seasonal differences (Figure 5). However, data distribution  
 297 indicates that the variability in NEE rate differs across different seasons, particularly between summer-  
 298 autumn and winter-spring. The changes in GPP over the two years were similar, with significant  
 299 differences observed between summer and winter ( $P < 0.05$ ). The RE was higher during summer-autumn  
 300 compared to winter-spring. The highest ecosystem respiration occurred in the first year during autumn,  
 301 while in the second year, it was highest during summer. Within the same year, summer and autumn  
 302 exhibited significant differences ( $P < 0.05$ ), while between the same seasons in different years, notable  
 303 distinctions were not observed. This pattern is also reflected in GPP and NEE.



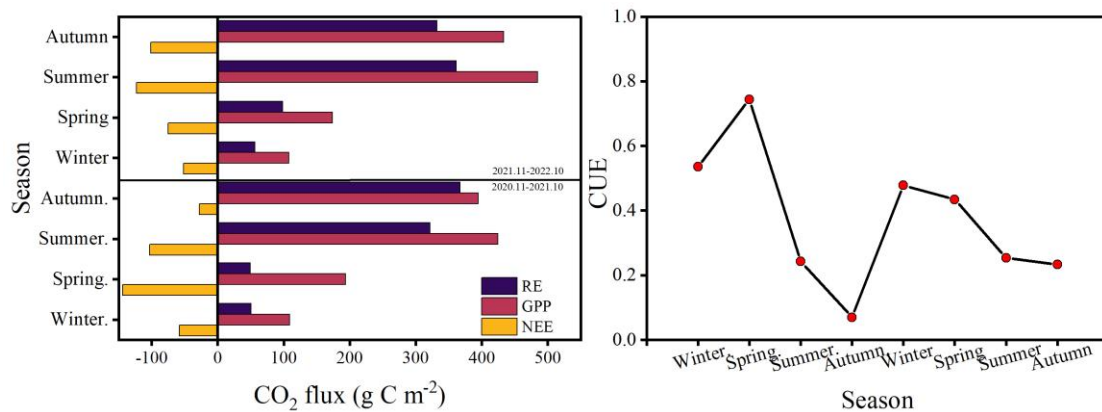
304

305 **Figure 5: Seasonal variation of CO<sub>2</sub> fluxes in two years.**

306

307 **3.5 Changes in total NEE, GPP, RE, and CUE**

308 The cumulative fluxes over the two years for the forest ecosystem are shown in Figure 6. NEE indicates  
 309 the net carbon sequestration in each month. The cumulative respiration reached its highest value of 361  
 310 g C m<sup>-2</sup> in the summer of 2022. The total NEE, GPP, and RE for the first year were -332, 1121, and 788  
 311 g C m<sup>-2</sup>, respectively, and -351, 1199, and 847 g C m<sup>-2</sup> for the second year, respectively. The CUE was  
 312 higher during the spring and lower during the autumn, with a maximum value of 0.74 and a minimum  
 313 value of 0.07. The average CUE over the two years was 0.40 and 0.35, respectively.



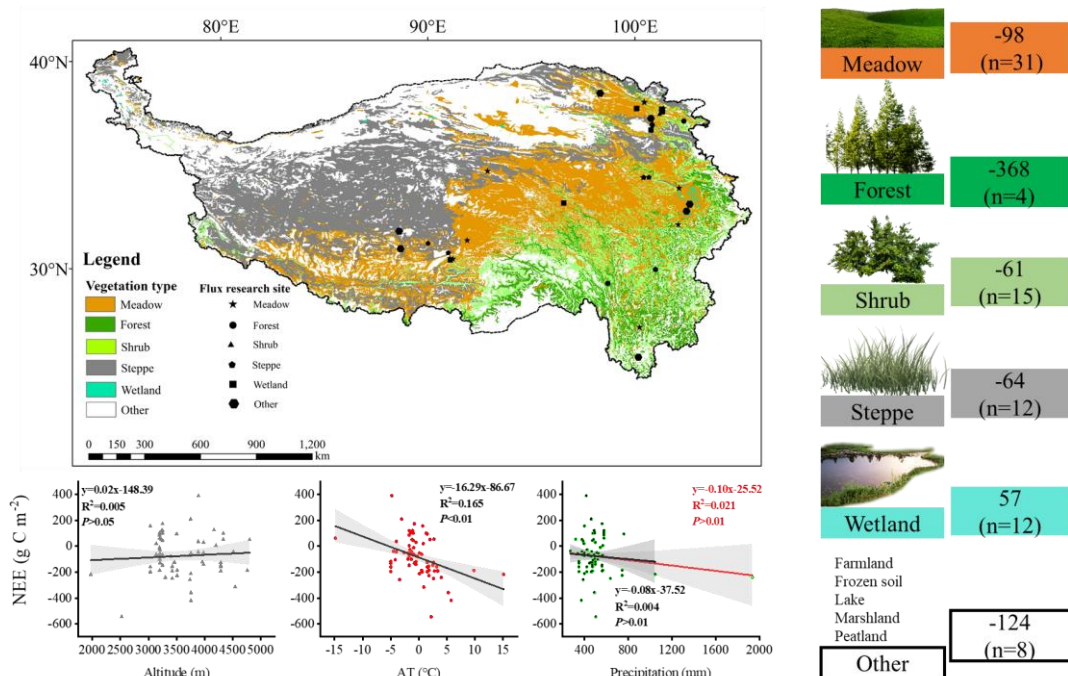
314

315 **Figure 6: Change in total carbon flux and carbon use efficiency.**

316

317 **3.6 The carbon sequestration potential of subalpine forests of QTP**

318 To clarify the carbon sequestration contribution of the subalpine forests found in the QTP, we compared  
 319 these research results (Figure 7). Found that ecosystems with high vegetation cover exhibited higher  
 320 annual cumulative carbon sequestration. Among these ecosystems, the subalpine forests in the QTP  
 321 showed the highest carbon sequestration potential, reaching an average of 368 g C m<sup>-2</sup> per year. The  
 322 carbon sequestration potential of different ecosystems ranked as follows: forest > meadow > steppe >  
 323 shrub. The average value for wetlands indicated that they are a significant source of CO<sub>2</sub>, releasing 57 g  
 324 C m<sup>-2</sup> into the atmosphere annually. We also analyzed the influence of altitude, mean annual air  
 325 temperature, and precipitation on NEE at these sites in the QTP. It has been observed that these sites  
 326 cover a wide range of altitudes, ranging from 1977 to 4800 m. According to existing results, an increase  
 327 in elevation may lead to a reduction in carbon uptake, while the range of mean annual temperature varies  
 328 between -14.8 to 15.1 °C, and higher mean annual temperatures significantly increase carbon uptake.  
 329 Forests exhibit the highest mean annual precipitation, averaging 827 mm, with mean annual precipitation  
 330 having a relatively weak impact on the NEE. These findings highlight the important role of subalpine  
 331 forests in carbon sequestration in the QTP and provide insights into the factors that affect carbon  
 332 exchange in the QTP, such as altitude, temperature, and precipitation.



333  
 334 **Figure 7: Carbon exchange potential of different ecosystems in the Qinghai-Tibet Plateau.**

335

336 **4 Discussion**

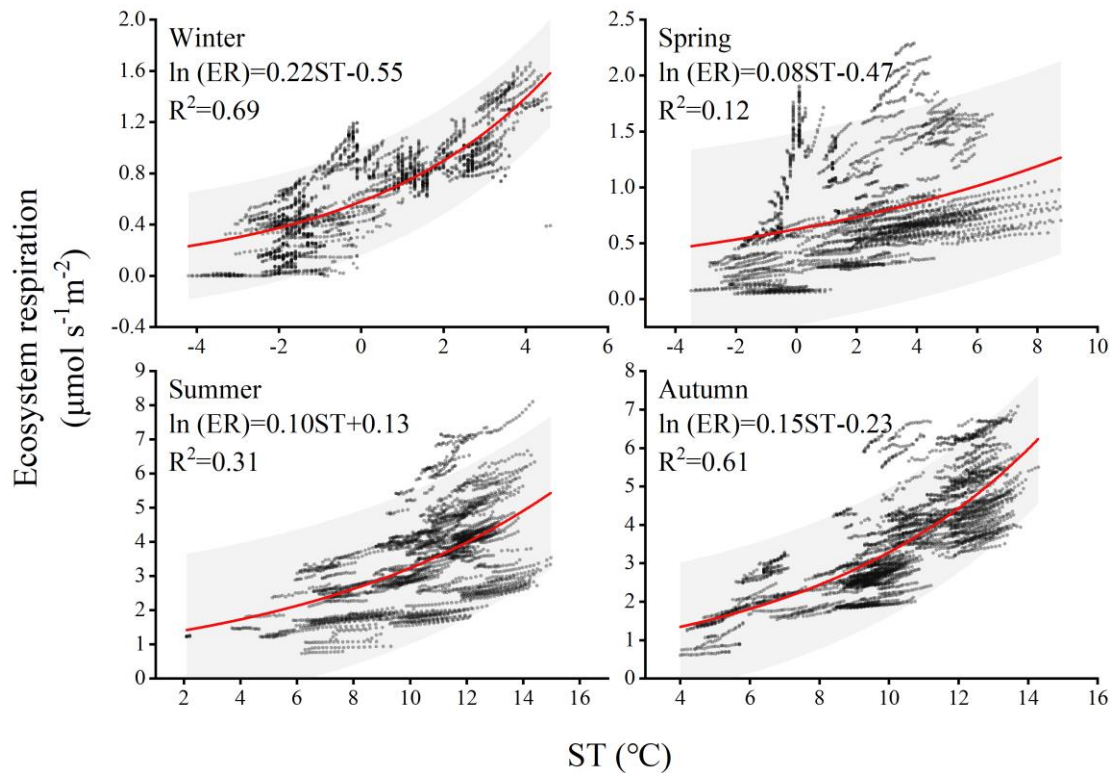
337 **4.1 Main factors affecting the carbon sequestration function of subalpine forests**

338 Climate change significantly affects the vegetation's carbon sequestration capacity, particularly at  
339 the seasonal scale due to phenological changes (Acosta-Hernández et al., 2020). In the short term,  
340 PAR, AT, RH, and VPD play important roles in regulating vegetation photosynthesis and,  
341 consequently, carbon uptake. For instance, PAR represents the portion of solar energy that can be  
342 utilized by plants and is an essential component in chloroplast reactions. PAR drives a nonlinear  
343 response of GPP to Solar-induced fluorescence (SIF) across different seasons, resulting in a strong  
344 positive correlation between GPP and SIF (Wang et al., 2023b). VPD affects photosynthesis and  
345 transpiration of leaves, with stomata serving as tiny pores mediating carbon dioxide uptake.  
346 Research has demonstrated that excessive increases in VPD are detrimental to photosynthesis. For  
347 instance, a moderate increase in VPD significantly reduces photosynthetic efficiency under light  
348 fluctuations, due to changes in RH and/or AT often accompanying fluctuations in light, studies also  
349 indicate that the impact of VPD on sunlight utilization efficiency is primarily determined by relative  
350 RH rather than AT (Liu et al., 2024). In different seasons, the same influencing factors exhibit  
351 varying degrees of contribution to NEE. For example, during winter, when the climatic conditions  
352 are relatively harsh with low air temperature and humidity, the forest maintains a low level of carbon  
353 uptake. On longer time scales, such as annual and decadal variations, the inherent changes in forest  
354 NEE may be attributed to disturbances and recovery (Hayek et al., 2018). In this study, significant  
355 differences in ecosystem respiration were observed during the summer and autumn in different years.  
356 Previous studies suggested that due to leaf aging or water stress, the photosynthetic light use  
357 efficiency of the ecosystem peaks after spring leaf expansion and gradually declines (Wehr et al.,  
358 2016). This implies a peak in carbon exchange during the summer, followed by higher productivity  
359 and ecosystem respiration in the following seasons. The variation in different years may be  
360 attributed to rainfall regulating the availability of natural resources such as water, biomass, litter,  
361 and soil nutrients (Schwinning and Sala, 2004). For instance, in temperate forests, when microbial  
362 biomass undergoes seasonal changes, microbial activity exhibits a seasonal lag in response to  
363 temperature variation, resulting in a seasonally delayed effect between litter heterotrophic  
364 respiration and temperature (Ataka et al., 2020). Whether such differences persist between different  
365 years on longer time scales remains to be demonstrated through more sustained and detailed

366 research in the future. Ecosystem respiration sensitivity to temperature is represented by the  $Q_{10}$   
367 coefficient. In this study, seasonal variations influenced the magnitude of  $Q_{10}$  (as shown in Figure 8).  
368 The calculated  $Q_{10}$  for each season are as follows: 9.03, 2.22, 2.71, and 4.48. The winter season exhibited  
369 the highest sensitivity of forest ecosystem respiration to temperature, indicating that respiration rates in  
370 the winter are more responsive to changes in temperature compared to other seasons. The main reason  
371 for such differences is that ecosystem respiration consists of heterotrophic respiration and autotrophic  
372 respiration, which are typically governed by different factors (Edwards, 1975). For instance, the high  
373 activity of soil microbes contributes to heterotrophic respiration, a process dominated by soil temperature  
374 and moisture conditions, which are severely restricted during the cold and dry conditions of winter (Falge  
375 et al., 2002). Simultaneously, due to the changing relative roles of growth and maintenance respiration,  
376 the allocation of autotrophic respiration varies seasonally. In winter, soil  $CO_2$  emissions constitute a  
377 significant portion of ecosystem  $CO_2$  emissions, and in some boreal forests, the ratio between the two  
378 can reach 0.6 or even higher (Davidson et al., 2006). In winter, under the frequent coverage of snow,  
379 cold-adapted microorganisms thriving in a relatively narrow sub-zero temperature range engage in  
380 respiration and exhibit relatively high sensitivity to warming or cooling beyond this range (Monson et  
381 al., 2006). The seasonal patterns of the  $Q_{10}$  value are jointly determined by the variation in the ratio of  
382 soil respiration to ecosystem respiration, reflecting these seasonal changes.

383 Our integrated analysis (as shown in Figure 7) reveals that despite the high elevation of the "Third Pole",  
384 the topographic factor of elevation does not have a significant impact on carbon uptake. Instead, NEE  
385 gradually increases with a steep rise in elevation. Research conducted by Wang et al. (2023c) has  
386 indicated that mean annual average temperature and precipitation are the main driving factors of  
387 interannual variations in NEE in alpine meadows and alpine steppes. Decreased precipitation resulted in  
388 a transition into carbon sources in some regions with high precipitation-dependent alpine grasslands. It  
389 is worth noting that, among all data collection sites, alpine wetlands show an average carbon source trend.  
390 Due to prolonged flooding and low temperatures, microbial activity in alpine wetlands is hindered, and  
391 the accumulation of organic carbon from plant litter decomposition is substantial. As a result,  
392 approximately  $57 \text{ g C m}^{-2}$  is emitted into the atmosphere annually. Previous studies have indicated that  
393 NEE in alpine wetlands is increasing with global warming (Yasin et al., 2022).





394  
 395 **Figure 8: Relationship between NEE night and soil temperature in different seasons.**

396  
 397 **4.2 Sustained carbon sequestration of subalpine forests**

398 Subalpine forests are integral components of global alpine ecosystems and play crucial roles in the global  
 399 carbon cycle. Our study on subalpine forests demonstrates a continuous absorption of carbon dioxide  
 400 even during winter, which aligns well with measurements taken in the vicinity of Mount Fuji in Japan  
 401 (Mizoguchi et al., 2012). The age of subalpine forests is a crucial factor influencing sustained carbon  
 402 sequestration. Based on NPP simulations of natural subalpine forests in the Northern Rockies, Carey  
 403 (2001) found that aboveground net primary productivity reaches its maximum after approximately 250  
 404 years, followed by a decline, this challenges the previous view that forests older than 100 years are  
 405 generally considered to be unimportant carbon sinks. Compared to the forest (mature forest) of Mount  
 406 Gongga in the QTP (e.g., Zhang et al., 2018), the subalpine forest in this study exhibits a stronger carbon  
 407 sequestration capacity. However, its carbon sequestration ability is slightly weaker than that of the Qilian  
 408 Mountains high-mountain forests (approximately 60-70 years old) in the QTP (Zhang et al., 2018; Du et  
 409 al., 2022b). Although existing flux monitoring results of high-altitude forests in the QTP indicate that  
 410 these forest ecosystems act as carbon sinks, it is important to consider that globally there are still many

411 cold regions with coniferous forests serving as carbon sources. For example, continuous CO<sub>2</sub> flux  
412 monitoring from native boreal forests in Sweden for over 10 years indicates that they are a net carbon  
413 source, which is attributed to the contribution of woody debris to RE due to disturbances such as extreme  
414 weather events, fires, insect infestations, and pathogen attacks (Hadden and Grelle, 2017). In the summer  
415 of 2018, Europe experienced a heatwave that affected the carbon cycling in forests. The mixed  
416 coniferous-deciduous forest in southern Estonian, under the influence of the heatwave, transitioned from  
417 a net carbon sink to a net carbon source in 2018 (Krasnova et al., 2022). Particular attention should be  
418 paid to the long-term monitoring in high-altitude environments of the impact of disturbances on forest  
419 carbon sequestration capacity. Our study has shown that forests in the QTP have the strongest carbon  
420 sink capacity, indicating that alpine forests will have an important sustained effect on carbon reduction  
421 in the QTP in the context of future climate change, but whether this sustained effect will be longer than  
422 other ecosystems is still unknown. However, a modeling experiment in a large semi-arid area of  
423 California predicted that grasslands are more resilient carbon sinks than forests in responding to climate  
424 change in the 21st century (Dass et al., 2018). In terms of carbon sequestration rate, forests in the QTP  
425 were significantly stronger than other ecosystems, followed by grasslands, while alpine deserts and  
426 alpine grasslands in the north-western and southern regions were the main carbon sources (Wu et al.,  
427 2022). Forests are mostly distributed in the south-eastern margin of the QTP and the mid-altitude area  
428 near 3000 m in the Sichuan-Tibet alpine gorge area, with an area of  $19.3 \times 10^4 \text{ km}^2$  (Wang et al., 2022b).  
429 Based on the average value of a few current carbon flux monitoring, the forest in the QTP will absorb  
430 about  $71 \times 10^6 \text{ Mg C year}^{-1}$ .

## 431 **5 Conclusion**

432 This study explores the carbon sequestration function, seasonal variations, and climate drivers of  
433 subalpine forests in the QTP. Over the observational period, we synchronously monitored ecosystem  
434 carbon exchange and primary environmental factors using an eddy covariance system. The research  
435 reveals that the subalpine forest acts as a carbon sink. Over the two years, the total NEE, GPP, and RE  
436 were  $-332$ ,  $1121$ , and  $788 \text{ g C m}^{-2}$  in first year, and  $-351$ ,  $1199$ , and  $847 \text{ g C m}^{-2}$  in second year.  
437 Photosynthetically active radiation was identified as the primary control of NEE, Relative humidity is  
438 negatively correlated with NEE, and its increase is not conducive to carbon sink. NEE reached its peak

439 in autumn. Combining results from other eddy covariance sites on the QTP, this study highlights that  
440 forests have the highest carbon sequestration potential, reaching  $368 \text{ g C m}^{-2}$  annually, followed by  
441 meadows ( $-98 \text{ g C m}^{-2}$ ), steppes ( $-64 \text{ g C m}^{-2}$ ), and shrubs ( $-61 \text{ g C m}^{-2}$ ). In contrast, wetlands were  
442 identified as a significant source of carbon dioxide ( $57 \text{ g C m}^{-2}$ ). Despite the challenges posed by climate  
443 change, the subalpine forests in the QTP retain substantial carbon sequestration potential. Strengthening  
444 conservation and management efforts for subalpine forests is crucial to ensure their continued and  
445 significant carbon sequestration function in the future. Overall, this research underscores the vital role of  
446 subalpine forests in the QTP as essential carbon sink regions, playing a critical role in the context of  
447 global climate change.

448 *Data availability.* The data is available from the authors on request.

449 *Authorship contributions.* Niu Zhu: Conceptualization, study design, data analyses, visualization,  
450 writing-original draft. JinNiu Wang: study design, writing—review & editing, supervision, project  
451 administration, funding acquisition. Dongliang Luo and Xufeng Wang: writing-reviewing & editing.  
452 Cheng Shen and Ning Wu: resources, data curation, supervision. all authors approved the final  
453 manuscript.

454 *Declaration of competing interest.* The authors declare that they have no conflict of interest.

455 *Acknowledgements.* We thank Ms. Neha Bisht for her substantial comments and language revision to  
456 improve the manuscript. This study was funded by CAS "Light of West China" Program (2021XBZG-  
457 XBQNXX-A-007); The National Natural Science Foundation of China (31971436); The State Key  
458 Laboratory of Cryospheric Science, Northwest Institute of Eco-Environment and Resources, Chinese  
459 Academy Sciences (SKLCS-OP-2021-06).

## 460 **Reference**

461 Acosta-Hernández, A. C., Padilla-Martínez, J. R., Hernández-Díaz, J. C., Prieto-Ruiz, J. A., Goche-Telles,  
462 J. R., Nájera-Luna, J. A., and Pompa-García, M.: Influence of Climate on Carbon Sequestration in  
463 Conifers Growing under Contrasting Hydro-Climatic Conditions, *Forests*, 11, 1134,  
464 <https://doi.org/10.3390/f11111134>, 2020.  
465 Ataka, M., Kominami, Y., Sato, K., and Yoshimura, K.: Microbial Biomass Drives Seasonal Hysteresis  
466 in Litter Heterotrophic Respiration in Relation to Temperature in a Warm-Temperate Forest, *Journal of*  
467 *Geophysical Research: Biogeosciences*, 125, e2020JG005729, <https://doi.org/10.1029/2020JG005729>,

468 2020.

469 Banbury Morgan, R., Herrmann, V., Kunert, N., Bond-Lamberty, B., Muller-Landau, H. C., and  
470 Anderson-Teixeira, K. J.: Global patterns of forest autotrophic carbon fluxes, *Global Change Biology*,  
471 27, 2840-2855, <https://doi.org/10.1111/gcb.15574>, 2021.

472 Baumgartner, S., Barthel, M., Drake, T. W., Bauters, M., Makelele, I. A., Mugula, J. K., Summerauer, L.,  
473 Gallarotti, N., Cizungu Ntaboba, L., Van Oost, K., Boeckx, P., Doetterl, S., Werner, R. A., and Six, J.:  
474 Seasonality, drivers, and isotopic composition of soil CO<sub>2</sub> fluxes from tropical forests of the Congo Basin,  
475 *Biogeosciences*, 17, 6207-6218, <https://doi.org/10.5194/bg-17-6207-2020>, 2020.

476 Cai, W., He, N., Li, M., Xu, L., Wang, L., Zhu, J., Zeng, N., Yan, P., Si, G., and Zhang, X.: Carbon  
477 sequestration of Chinese forests from 2010 to 2060: Spatiotemporal dynamics and its regulatory  
478 strategies, *Science Bulletin*, 67, 836-843, <https://doi.org/10.1016/j.scib.2021.12.012>, 2022.

479 Cao, S., Cao, G., Chen, K., Han, G., Liu, Y., Yang, Y., and Li, X.: Characteristics of CO<sub>2</sub>, water vapor,  
480 and energy exchanges at a headwater wetland ecosystem of the Qinghai Lake, *Canadian Journal of Soil  
481 Science*, 99, 227-243, <https://doi.org/10.1139/cjss-2018-0104>, 2019.

482 Carey, E. V., Sala, A., Keane, R., and Callaway, R. M.: Are old forests underestimated as global carbon  
483 sinks?, *Global Change Biology*, 7, 339-344, <https://doi.org/10.1046/j.1365-2486.2001.00418.x>, 2001.

484 Chen, H., Ju, P. J., Zhu, Q., Xu, X. L., Wu, N., Gao, Y. H., Feng, X. J., Tian, J. Q., Niu, S. L., Zhang, Y.  
485 J., Peng, C. H., and Wang, Y. F.: Carbon and nitrogen cycling on the Qinghai-Tibetan Plateau, *Nature  
486 Reviews Earth & Environment*, 3, 701-716, <https://doi.org/10.1038/s43017-022-00344-2>, 2022.

487 Cole, J. J., Caraco, N. F., Kling, G. W., and Kratz, T. K.: Carbon dioxide supersaturation in the surface  
488 waters of lakes, *Science*, 265, 1568-1570, <https://doi.org/10.1126/science.265.5178.1568>, 1994.

489 Dass, P., Houlton, B. Z., Wang, Y., and Warlind, D.: Grasslands may be more reliable carbon sinks than  
490 forests in California, *Environmental Research Letters*, 13, 074027, [10.1088/1748-9326/aacb39](https://doi.org/10.1088/1748-9326/aacb39), 2018.

491 Davidson, E. A., Richardson, A. D., Savage, K. E., and Hollinger, D. Y.: A distinct seasonal pattern of  
492 the ratio of soil respiration to total ecosystem respiration in a spruce-dominated forest, *Global Change  
493 Biology*, 12, 230-239, <https://doi.org/10.1111/j.1365-2486.2005.01062.x>, 2006.

494 Du, C., Zhou, G., and Gao, Y.: Grazing exclusion alters carbon flux of alpine meadow in the Tibetan  
495 Plateau, *Agricultural and Forest Meteorology*, 314, 108774,  
496 <https://doi.org/10.1016/j.agrformet.2021.108774>, 2022a.

497 Du, Y., Pei, W., Zhou, H., Li, J., Wang, Y., and Chen, K.: Net ecosystem exchange of carbon dioxide  
498 fluxes and its driving mechanism in the forests on the Tibetan Plateau, *Biochemical Systematics and*  
499 *Ecology*, 103, <https://doi.org/10.1016/j.bse.2022.104451>, 2022b.

500 Ebermayer, E.: Die gesammte Lehre der Waldstreu mit Rücksicht auf die chemische Statik des  
501 Waldbaues: unter Zugrundlegung der in den Königl. Staatsforsten Bayerns angestellten Untersuchungen,  
502 ISBN 3642896340, Springer 1876.

503 Edwards, N. T.: Effects of Temperature and Moisture on Carbon Dioxide Evolution in a Mixed Deciduous  
504 Forest Floor, *Soil Science Society of America Journal*, 39, 361-365,  
505 <https://doi.org/10.2136/sssaj1975.03615995003900020034x>, 1975.

506 Falge, E., Baldocchi, D., Tenhunen, J., Aubinet, M., Bakwin, P., Berbigier, P., Bernhofer, C., Burba, G.,  
507 Clement, R., Davis, K. J., Elbers, J. A., Goldstein, A. H., Grelle, A., Granier, A., Guðmundsson, J.,  
508 Hollinger, D., Kowalski, A. S., Katul, G., Law, B. E., Malhi, Y., Meyers, T., Monson, R. K., Munger, J.  
509 W., Oechel, W., Paw U, K. T., Pilegaard, K., Rannik, Ü., Rebmann, C., Suyker, A., Valentini, R., Wilson,  
510 K., and Wofsy, S.: Seasonality of ecosystem respiration and gross primary production as derived from  
511 FLUXNET measurements, *Agricultural and Forest Meteorology*, 113, 53-74,  
512 [https://doi.org/10.1016/S0168-1923\(02\)00102-8](https://doi.org/10.1016/S0168-1923(02)00102-8), 2002.

513 Falge, E., Baldocchi, D., Olson, R., Anthoni, P., Aubinet, M., Bernhofer, C., Burba, G., Ceulemans, R.,  
514 Clement, R., Dolman, H., Granier, A., Gross, P., Grünwald, T., Hollinger, D., Jensen, N.-O., Katul, G.,  
515 Keronen, P., Kowalski, A., Lai, C. T., Law, B. E., Meyers, T., Moncrieff, J., Moors, E., Munger, J. W.,  
516 Pilegaard, K., Rannik, Ü., Rebmann, C., Suyker, A., Tenhunen, J., Tu, K., Verma, S., Vesala, T., Wilson,  
517 K., and Wofsy, S.: Gap filling strategies for defensible annual sums of net ecosystem exchange,  
518 *Agricultural and Forest Meteorology*, 107, 43-69, [https://doi.org/10.1016/S0168-1923\(00\)00225-2](https://doi.org/10.1016/S0168-1923(00)00225-2), 2001.

519 Foken, T., Göockede, M., Mauder, M., Mahrt, L., Amiro, B., and Munger, W.: Post-Field Data Quality  
520 Control, in: *Handbook of Micrometeorology: A Guide for Surface Flux Measurement and Analysis*,  
521 edited by: Lee, X., Massman, W., and Law, B., Springer Netherlands, Dordrecht, 181-208,  
522 [https://doi.org/10.1007/1-4020-2265-4\\_9](https://doi.org/10.1007/1-4020-2265-4_9), 2005.

523 Hadden, D. and Grelle, A.: Net CO<sub>2</sub> emissions from a primary boreo-nemoral forest over a 10 year period,  
524 *Forest Ecology and Management*, 398, 164-173, <https://doi.org/10.1016/j.foreco.2017.05.008>, 2017.

525 Hayek, M. N., Longo, M., Wu, J., Smith, M. N., Restrepo-Coupe, N., Tapajos, R., da Silva, R., Fitzjarrald,

526 D. R., Camargo, P. B., Hutrya, L. R., Alves, L. F., Daube, B., Munger, J. W., Wiedemann, K. T., Saleska,  
527 S. R., and Wofsy, S. C.: Carbon exchange in an Amazon forest: from hours to years, *Biogeosciences*, 15,  
528 4833-4848, <https://doi.org/10.5194/bg-15-4833-2018>, 2018.

529 Jia, X., Mu, Y., Zha, T., Wang, B., Qin, S., and Tian, Y.: Seasonal and interannual variations in ecosystem  
530 respiration in relation to temperature, moisture, and productivity in a temperate semi-arid shrubland,  
531 *Science of The Total Environment*, 709, 136210, <https://doi.org/10.1016/j.scitotenv.2019.136210>, 2020.

532 KATO, T., TANG, Y., GU, S., HIROTA, M., DU, M., LI, Y., and ZHAO, X.: Temperature and biomass  
533 influences on interannual changes in CO<sub>2</sub> exchange in an alpine meadow on the Qinghai-Tibetan Plateau,  
534 *Global Change Biology*, 12, 1285-1298, <https://doi.org/10.1111/j.1365-2486.2006.01153.x>, 2006.

535 Kondo, M., Saitoh, T. M., Sato, H., and Ichii, K.: Comprehensive synthesis of spatial variability in carbon  
536 flux across monsoon Asian forests, *Agricultural and Forest Meteorology*, 232, 623-634,  
537 <https://doi.org/10.1016/j.agrformet.2016.10.020>, 2017.

538 Konopka, J., Heusinger, J., and Weber, S.: Extensive Urban Green Roof Shows Consistent Annual Net  
539 Uptake of Carbon as Documented by 5 Years of Eddy-Covariance Flux Measurements, *Journal of*  
540 *Geophysical Research: Biogeosciences*, 126, e2020JG005879, <https://doi.org/10.1029/2020JG005879>,  
541 2021.

542 Krasnova, A., Mander, Ü., Noe, S. M., Uri, V., Krasnov, D., and Soosaar, K.: Hemiboreal forests' CO<sub>2</sub>  
543 fluxes response to the European 2018 heatwave, *Agricultural and Forest Meteorology*, 323, 109042,  
544 <https://doi.org/10.1016/j.agrformet.2022.109042>, 2022.

545 Landsberg, J. and Waring, R.: A generalised model of forest productivity using simplified concepts of  
546 radiation-use efficiency, carbon balance and partitioning, *Forest ecology and management*, 95, 209-228,  
547 [https://doi.org/10.1016/S0378-1127\(97\)00026-1](https://doi.org/10.1016/S0378-1127(97)00026-1), 1997.

548 Laurin, G. V., Chen, Q., Lindsell, J. A., Coomes, D. A., Del Frate, F., Guerriero, L., Pirotti, F., and  
549 Valentini, R.: Above ground biomass estimation in an African tropical forest with lidar and hyperspectral  
550 data, *ISPRS Journal of Photogrammetry and Remote Sensing*, 89, 49-58,  
551 <https://doi.org/10.1016/j.isprsjprs.2014.01.001>, 2014.

552 Leuning, R. and King, K. M.: Comparison of eddy-covariance measurements of CO<sub>2</sub> fluxes by open-  
553 and closed-path CO<sub>2</sub> analysers, *Boundary-Layer Meteorology*, 59, 297-311,  
554 <https://doi.org/10.1007/BF00119818>, 1992.

555 Li, L., Zhang, Y., Wu, J., Li, S., Zhang, B., Zu, J., Zhang, H., Ding, M., and Paudel, B.: Increasing  
556 sensitivity of alpine grasslands to climate variability along an elevational gradient on the Qinghai-Tibet  
557 Plateau, *Science of the Total Environment*, 678, 21-29, <https://doi.org/10.1016/j.scitotenv.2019.04.399>,  
558 2019.

559 Li, X. Y., Shi, F. Z., Ma, Y. J., Zhao, S. J., and Wei, J. Q.: Significant winter CO<sub>2</sub> uptake by saline lakes  
560 on the Qinghai-Tibet Plateau, *Global Change Biology*, 28, 2041-2052, <https://doi.org/10.1111/gcb.16054>,  
561 2022.

562 Liu, C., Wu, Z., Hu, Z., Yin, N., Islam, A. T., and Wei, Z.: Characteristics and influencing factors of  
563 carbon fluxes in winter wheat fields under elevated CO<sub>2</sub> concentration, *Environmental Pollution*, 307,  
564 119480, <https://doi.org/10.1016/j.envpol.2022.119480>, 2022.

565 Liu, J., Zou, H.-X., Bachelot, B., Dong, T., Zhu, Z., Liao, Y., Plenković-Moraj, A., and Wu, Y.: Predicting  
566 the responses of subalpine forest landscape dynamics to climate change on the eastern Tibetan Plateau,  
567 *Global Change Biology*, 27, 4352-4366, <https://doi.org/10.1111/gcb.15727>, 2021.

568 Liu, N.-Y., Yang, Q.-Y., Wang, J.-H., Zhang, S.-B., Yang, Y.-J., and Huang, W.: Differential Effects of  
569 Increasing Vapor Pressure Deficit on Photosynthesis at Steady State and Fluctuating Light, *Journal of*  
570 *Plant Growth Regulation*, <https://doi.org/10.1007/s00344-024-11268-0>, 2024.

571 Lloyd, J. and Taylor, J. A.: On the temperature dependence of soil respiration, *Functional Ecology*, 8,  
572 315-323, <https://doi.org/10.2307/2389824>, 1994.

573 Mamkin, V., Avilov, V., Ivanov, D., Varlagin, A., and Kurbatova, J.: Interannual variability in the  
574 ecosystem CO<sub>2</sub> fluxes at a paludified spruce forest and ombrotrophic bog in the southern taiga,  
575 *Atmospheric Chemistry and Physics*, 23, 2273-2291, <https://doi.org/10.5194/acp-23-2273-2023>, 2023.

576 Mao, D., Luo, L., Wang, Z., Zhang, C., and Ren, C.: Variations in net primary productivity and its  
577 relationships with warming climate in the permafrost zone of the Tibetan Plateau, *Journal of*  
578 *Geographical Sciences*, 25, 967-977, <https://doi.org/10.1007/s11442-015-1213-8>, 2015.

579 Mauder, M. and Foken, T.: Documentation and Instruction Manual of the Eddy-Covariance Software  
580 Package TK3 (update), 2011.

581 Mizoguchi, Y., Ohtani, Y., Takahashi, S., Iwata, H., Yasuda, Y., and Nakai, Y.: Seasonal and interannual  
582 variation in net ecosystem production of an evergreen needleleaf forest in Japan, *Journal of Forest*  
583 *Research*, 17, 283-295, <https://doi.org/10.1007/s10310-011-0307-0>, 2012.

584 Moncrieff, J. B., Massheder, J. M., de Bruin, H., Elbers, J., Friborg, T., Heusinkveld, B., Kabat, P., Scott,  
585 S., Soegaard, H., and Verhoef, A.: A system to measure surface fluxes of momentum, sensible heat, water  
586 vapour and carbon dioxide, *Journal of Hydrology*, 188-189, 589-611, [https://doi.org/10.1016/S0022-](https://doi.org/10.1016/S0022-1694(96)03194-0)  
587 1694(96)03194-0, 1997.

588 Monson, R. K., Lipson, D. L., Burns, S. P., Turnipseed, A. A., Delany, A. C., Williams, M. W., and  
589 Schmidt, S. K.: Winter forest soil respiration controlled by climate and microbial community  
590 composition, *Nature*, 439, 711-714, <https://doi.org/10.1038/nature04555>, 2006.

591 Monteith, J. L., Unsworth, M. H., and Webb, A.: Principles of environmental physics, *Quarterly Journal*  
592 *of the Royal Meteorological Society*, 120, 1699, <https://doi.org/10.1002/qj.49712052015>, 1994.

593 Mu, C., Mu, M., Wu, X., Jia, L., Fan, C., Peng, X., Ping, C. I., Wu, Q., Xiao, C., and Liu, J.: High carbon  
594 emissions from thermokarst lakes and their determinants in the Tibet Plateau, *Global Change Biology*,  
595 29(10), 2732–2745, <https://doi.org/10.1111/gcb.16658> 2023.

596 Niu, Z., Jinniu, W., Xufeng, W., Dongliang, L., Cheng, S., and Aihong, G.: Net ecosystem CO<sub>2</sub> exchange  
597 and its influencing factors in non-growing season at a sub-alpine forest in the core Three Parallel Rivers  
598 region, *Acta Ecologica Sinica*, 43, 5967-5979, <https://doi.org/10.5846/stxb202204020841>, 2023.(in  
599 Chinese)

600 Organization, W. M.: 2019 concludes a decade of exceptional global heat and high-  
601 impactweather[EB/OL].[https://public.wmo.int/en/media/press-release/2019-concludes-decade-of-](https://public.wmo.int/en/media/press-release/2019-concludes-decade-of-exceptional-global-heat-and-high-impact-weather)  
602 exceptional-global-heat-and-high-impact-weather, 2019.

603 Pan, Y., Birdsey, R. A., Fang, J., Houghton, R., Kauppi, P. E., Kurz, W. A., Phillips, O. L., Shvidenko, A.,  
604 Lewis, S. L., and Canadell, J. G.: A large and persistent carbon sink in the world's forests, *Science*, 333,  
605 988-993, <https://doi.org/10.1126/science.120160>, 2011.

606 Pavelka, M., Acosta, M., Marek, M. V., Kutsch, W., and Janous, D.: Dependence of the Q10 values on  
607 the depth of the soil temperature measuring point, *Plant and Soil*, 292, 171-179,  
608 <https://doi.org/10.1007/s11104-007-9213-9>, 2007.

609 Qu, S., Xu, R., Yu, J., and Borjigidai, A.: Extensive atmospheric methane consumption by alpine forests  
610 on Tibetan Plateau, *Agricultural and Forest Meteorology*, 339, 109589,  
611 <https://doi.org/10.1016/j.agrformet.2023.109589>, 2023.

612 Reichstein, M., Falge, E., Baldocchi, D., Papale, D., Aubinet, M., Berbigier, P., Bernhofer, C., Buchmann,



613 N., Gilmanov, T., Granier, A., Grünwald, T., Havránková, K., Ilvesniemi, H., Janous, D., Knohl, A.,  
614 Laurila, T., Lohila, A., Loustau, D., Matteucci, G., Meyers, T., Miglietta, F., Ourcival, J.-M., Pumpanen,  
615 J., Rambal, S., Rotenberg, E., Sanz, M., Tenhunen, J., Seufert, G., Vaccari, F., Vesala, T., Yakir, D., and  
616 Valentini, R.: On the separation of net ecosystem exchange into assimilation and ecosystem respiration:  
617 review and improved algorithm, *Global Change Biology*, 11, 1424-1439, [https://doi.org/10.1111/j.1365-](https://doi.org/10.1111/j.1365-2486.2005.001002.x)  
618 2486.2005.001002.x, 2005.

619 Schotanus, P., Nieuwstadt, F. T. M., and De Bruin, H. A. R.: Temperature measurement with a sonic  
620 anemometer and its application to heat and moisture fluxes, *Boundary-Layer Meteorology*, 26, 81-93,  
621 <https://doi.org/10.1007/BF00164332>, 1983.

622 Schweizer, V. J., Ebi, K. L., van Vuuren, D. P., Jacoby, H. D., Riahi, K., Strefler, J., Takahashi, K., van  
623 Ruijven, B. J., and Weyant, J. P.: Integrated Climate-Change Assessment Scenarios and Carbon Dioxide  
624 Removal, *One Earth*, 3, 166-172, <https://doi.org/10.1016/j.oneear.2020.08.001>, 2020.

625 Schwinning, S. and Sala, O. E.: Hierarchy of responses to resource pulses in arid and semi-arid  
626 ecosystems, *Oecologia*, 141, 211-220, <https://doi.org/10.1007/s00442-004-1520-8>, 2004.

627 Stein, T.: Carbon dioxide peaks near 420 parts per million at Mauna Loa observatory, NOAA Research,  
628 June, 7, <https://research.noaa.gov/2021/06/07>, 2021.

629 Tang, X., Xiao, J., Ma, M., Yang, H., Li, X., Ding, Z., Yu, P., Zhang, Y., Wu, C., Huang, J., and Thompson,  
630 J. R.: Satellite evidence for China's leading role in restoring vegetation productivity over global karst  
631 ecosystems, *Forest Ecology and Management*, 507, 120000,  
632 <https://doi.org/10.1016/j.foreco.2021.120000>, 2022.

633 Vote, C., Hall, A., and Charlton, P.: Carbon dioxide, water and energy fluxes of irrigated broad-acre crops  
634 in an Australian semi-arid climate zone, *Environmental Earth Sciences*, 73, 449-465,  
635 <https://doi.org/10.1007/s12665-014-3547-4>, 2015.

636 Wang, C.-Y., Wang, J.-N., Wang, X.-F., Luo, D.-L., Wei, Y.-Q., Cui, X., Wu, N., and Bagaria, P.:  
637 Phenological Changes in Alpine Grasslands and Their Influencing Factors in Seasonally Frozen Ground  
638 Regions Across the Three Parallel Rivers Region, Qinghai-Tibet Plateau, *Frontiers in Earth Science*, 9,  
639 <https://doi.org/10.3389/feart.2021.797928>, 2022a.

640 Wang, S., Grant, R., Verseghy, D., and Black, T.: Modelling plant carbon and nitrogen dynamics of a  
641 boreal aspen forest in CLASS—the Canadian Land Surface Scheme, *Ecological Modelling*, 142, 135-

642 154, [https://doi.org/10.1016/S0304-3800\(01\)00284-8](https://doi.org/10.1016/S0304-3800(01)00284-8), 2001.

643 Wang, Y., Yao, G., Zuo, Y., and Wu, Q.: Implications of global carbon governance for corporate carbon  
644 emissions reduction, *Frontiers in Environmental Science*, 11, 3,  
645 <https://doi.org/10.3389/fenvs.2023.1071658>, 2023a.

646 Wang, Y., Sun, Y., Chen, Y., Wu, C., Huang, C., Li, C., and Tang, X.: Non-linear correlations exist  
647 between solar-induced chlorophyll fluorescence and canopy photosynthesis in a subtropical evergreen  
648 forest in Southwest China, *Ecological Indicators*, 157, 111311,  
649 <https://doi.org/10.1016/j.ecolind.2023.111311>, 2023b.

650 Wang, Y., Xiao, J., Ma, Y., Ding, J., Chen, X., Ding, Z., and Luo, Y.: Persistent and enhanced carbon  
651 sequestration capacity of alpine grasslands on Earth's Third Pole, *Science Advances*, 9,  
652 eade6875, <https://doi.org/10.1126/sciadv.ade6875>, 2023c.

653 Wang, Y., Xiao, J., Ma, Y., Luo, Y., Hu, Z., Li, F., Li, Y., Gu, L., Li, Z., and Yuan, L.: Carbon fluxes and  
654 environmental controls across different alpine grassland types on the Tibetan Plateau, *Agricultural and  
655 Forest Meteorology*, 311, 108694, <https://doi.org/10.1016/j.agrformet.2021.108694>, 2021.

656 Wang, Z. Y., Li, Z. Y., Dong, S. K., Fu, M. L., Li, Y. S., Li, S. M., Wu, S. N., Ma, C. H., Ma, T. X., and  
657 Cao, Y.: Evolution of ecological patterns and its driving factors on Qinghai-Tibet Plateau over the past  
658 40 years, *Acta Ecologica Sinica*, 42, 8941-8952, <https://doi.org/10.5846/stxb202204191060>, 2022b.(in  
659 Chinese)

660 Wehr, R., Munger, J. W., McManus, J. B., Nelson, D. D., Zahniser, M. S., Davidson, E. A., Wofsy, S. C.,  
661 and Saleska, S. R.: Seasonality of temperate forest photosynthesis and daytime respiration, *Nature*, 534,  
662 680-683, <https://doi.org/10.1038/nature17966>, 2016.

663 Wu, T., Ma, W., Wu, X., Li, R., Qiao, Y., Li, X., Yue, G., Zhu, X., and Ni, J.: Weakening of carbon sink  
664 on the Qinghai-Tibet Plateau, *Geoderma*, 412, 115707, <https://doi.org/10.1016/j.geoderma.2022.115707>,  
665 2022.

666 Yasin, A., Niu, B., Chen, Z., Hu, Y., Yang, X., Li, Y., Zhang, G., Li, F., and Hou, W.: Effect of warming  
667 on the carbon flux of the alpine wetland on the Qinghai-Tibet Plateau, *Frontiers in Earth Science*, 10,  
668 <https://doi.org/10.3389/feart.2022.935641>, 2022.

669 YU, G. and SUN, X.: Principles of flux measurement in terrestrial ecosystem, Beijing: Higher Education  
670 Press, ISBN 978-7-04-046012-42006. (in Chinese)

671 Yu, Y.: Double-order system construction of China's climate change legislation under the dual carbon  
672 goals, *China Population Resources and Environment*, 32, 89-96, [https://doi.org/10.12062/cpre.](https://doi.org/10.12062/cpre.20211120)  
673 20211120, 2022. (in Chinese)

674 Zemin, Z., Fenggui, L., Qiong, C., Xingsheng, X., and Qiang, Z.: Spatial Prediction of Potential Property  
675 Loss by Geological Hazards based on Random Forest—A Case Study of Chamdo, Tibet, *Plateau Science*  
676 *Research*, 7, 21-30, <https://doi.org/10.16249/j.cnki.2096-4617.2023.02.003>, 2023.

677 Zhang, J., Lin, H., Li, S., Yang, E., Ding, Y., Bai, Y., and Zhou, Y.: Accurate gas extraction (AGE) under  
678 the dual-carbon background: Green low-carbon development pathway and prospect, *Journal of Cleaner*  
679 *Production*, 134372, <https://doi.org/10.1016/j.jclepro.2022.134372>, 2022.

680 Zhang, Y., Zhu, W., Sun, X., and Hu, Z.: Carbon dioxide flux characteristics in an *Abies fabri* mature  
681 forest on Gongga Mountain, Sichuan, China, *Acta Ecologica Sinica*, 38, 6125-6135,  
682 [https://doi.org/10.5846 / stxb2017090515992](https://doi.org/10.5846/stxb2017090515992), 018. (in Chinese)

683